Hybrid Energy Storage For Microgrid Performance Improvement Under unbalanced load Conditions

SALMAN HAJIAGHASI[1,*], AHMAD SALEMNIA[1], AND MOHSEN HAMZEH[1]

[1] Faculty of Electrical Engineering, Shahid Beheshti Univercity, A.C, Tehran, Iran
[*] Corresponding author: S_Hajiaghasi@sbu.ac.ir

Manuscript received February 19, 2018; revised April 04: accepted April 12, 2018. Paper no. JEMT1802-1065

Energy storage system (ESS) is generally used to manage the intermittency of renewable energy sources (RESs). One of the important issues in microgrids, is to supply high quality powers to consumers. This paper proposes the use of hybrid energy storages to improve the power quality under unbalanced load conditions for microgrids applications. Battery and Supercapacitor (SC) are used as hybrid energy storages systems (HESSs) that provide low and high power frequency respectively. The proportional resonance(PR) and fuzzy controllers are, respectively, used to regulate the AC load voltage and DC bus voltage controller. The main advantages of the proposed energy management scheme are to reduce battery power fluctuations, better DC bus voltage regulation for generation and load disturbances, improvement of the system performance under unbalanced load conditions, reduced rate of charge/discharge of battery current, improved power quality feature under unbalanced load and transition conditions. The performance of the proposed method and control strategy is verified by using simulation studies in the MATLAB software environment.

keywords: *Hybrid Storage; Battery; Supercapacitor; Unbalanced Load; Proportional Resonance.*

http://dx.doi.org/10.22109/jemt.2018.109536.1065

1. INTRODUCTION

With world electricity activity growing steadily, the demand for renewable energy sources (RES) is also expected to increase drastically. Microgrids emerged as a solution to RES connection to load and grid [1]. Microgrids are electricity distribution systems containing loads and distributed energy resources, such as distributed generators, storage devices, or controllable loads, that can be operated in a controlled and coordinated way either while connected to the main power network or while is landed. A dedicated ESS could contribute to a better integration of RES into the microgrid by smoothing the renewable resource's intermittency, improving the quality of the injected power and enabling additional services like voltage and frequency regulation [2]. A single technology ESS has limited characteristics in terms of cost, lifetime, power and energy density, depending on the energy storage technology it uses [3], therefore, HESSs have been proposed to overcome these limits by harnessing the advantages of different energy storage technologies. Depending on the performance characteristics of an energy storage technology, it can be ideal for certain power system services and less suitable for other applications [4]. Fig.1 depicts the most important storage technologies for the microgrids [5]. Battery and SC combination is one of the attracting HESS configurations. The SC has a greater power density than the battery, allowing the SC to provide more power over a shorter period of time. Conversely, the battery has a higher energy density compared to the SC to supply the lower power for a longer period of time. When make a comparison between SCs and batteries, following results are obtained: batteries have high energy density changing between 120Wh/kg and 200Wh/kg; but they have low power density. SCs have high power density changing between 2kW/kg and

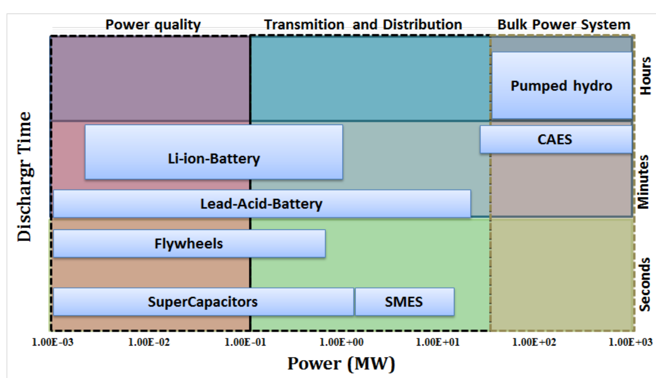

Fig. 1. Various storages technology comparison [5].

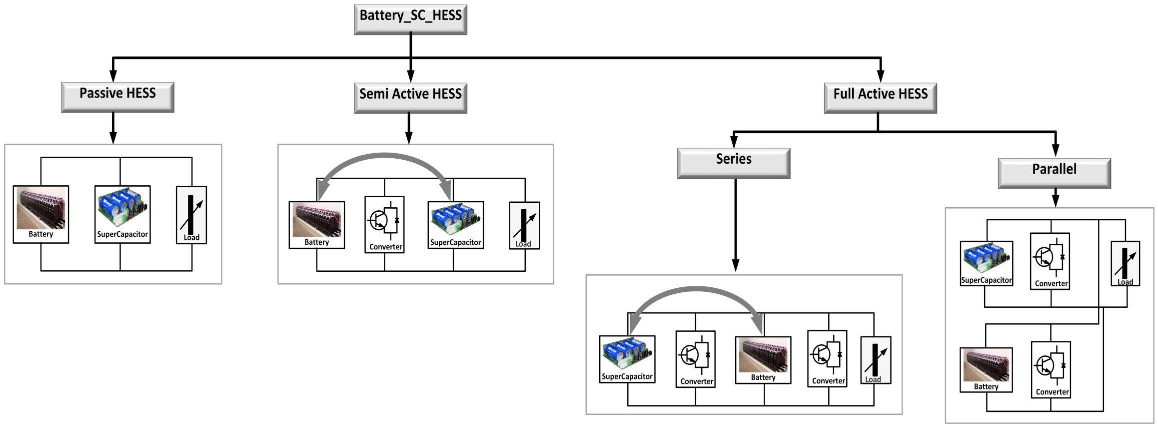

Fig. 2. battery-SC topology for connection with power electronic converter.

5kW/kg; but they have low energy density. The lifetime of the battery depends on several parameters, i.e., temperature, the number of peak currents, charge and discharge cycles, high frequency ripple current etc [6].

HESS can be categorized based on their connection topology as passive, active and semi active [7] that are shown in Fig.2. In the passive design, the battery and SC packs are connected in parallel and directly coupled to the DC bus [8]. The semi-active topology adds a power electronic converter between the SC or Battery and the DC bus, while the battery is directly connected to the DC bus [9]. The best control can be implemented in a fully active HESS and is the most commonly used configuration. The advantage of this configuration is that both the current from the battery and the current from the SC can be controlled actively [10].

For a microgrid, it is important to supply high quality powers to consumers. In practice, various types of loads such as unbalanced and non linear loads are supplied by a microgrid system. Nevertheless, a microgrid should be able to operate under all load conditions without any performance degradations. In recent years, the battery-SC based HESS has been proposed to mitigate the impact of dynamic power exchanges on battery's lifespan. HESS have been used in microgrids for various purposes. The strategy of regulation of the hybrid storage DC bus voltage has been presented in [11]. SCs are used to reduce stresses on batteries and improve their life cycle. The performance of the root mean square(RMS) current gain in battery, the gain in energy losses, the total energy efficiency and the elimination rate of surge load power are also explored, in different operating state conditions. In [12], [13] the joint control strategy is proposed for photovoltaic (PV) based DC grid system, with battery and SC as a HESS. Control strategy utilizes the uncompensated power from the battery system to increase the performance of the overall HESS. Unlike the conventional methods which only use either filtration based controller (FBC) or fuzzy logic controller (FLC), the proposed control strategy in [14] comprises of a low-pass filter (LPF) and FLC. Firstly, LPF removes the high dynamic components from the battery demand. FLC minimizes the battery peak current demand while constantly considering the state-of-charge of the SC.

Unbalanced loads are one of the problem of electrical networks and microgrids [15]. When an unbalanced load added to the system, three phase voltage lose their symmetry and power quality reduces. PR controllers are used as a solution to unbalanced load [16]. Using PR controller, voltages remain balanced but currents become unbalanced. In [17], according to the HESS, a coordination control strategy is proposed to enhance the power quality of microgrid under unbalanced load conditions. The HESS is composed of a lithium battery power conversion system and an ultra-capacitor power conversion system. In [18], a second order sliding mode controller is proposed for the power flow control of a HESS, using a four leg three level neutral point clamped (4-Leg 3LNPC) inverter as the only interface between the RES/HESS and the microgrid.

The output voltage of RES and storages is often DC, so they are connected to grid by power electronic converters. Unbalanced loads case distortion of DC bus current. Distorted current is passing through power generation units and storages. The main disadvantages of distortion current are: 1) distorted dc bus voltage 2) distortion of generation currents 3) storages currents distortion 4) increased battery current stress 5) increase in battery charge and discharge cycle 6) reduction in battery lifespan. To solve the problems mentioned, the use of HESS is proposed in this paper which has not been done in previous researches. Battery and SC are used as energy storages in an islanded microgrid to improve system performance under unbalanced load conditions. To compensate unbalanced voltage at the AC side, PR controller is used for current and voltage controllers. To improve system performance under unbalanced conditions, load changes and transient conditions, fuzzy-PI controller are used to control the DC bus voltage. The main contributions of this paper are battery life extension, system performance improvement and better response to system dynamics under unbalanced load conditions. Power and life extension of battery- SC hybrids increase the performance of the battery by preventing its action with high frequency ripple currents and high rate of depth of discharge to increase the battery lifetime to prolong the battery lifetime by minimizing battery current magnitude and variations. The voltage ripple coupled to highly unbalanced AC loads may cause large dc current harmonics which may increase electro- magnetic interference and impact battery lifetime due to increased thermal losses. The remaining of this paper is organized as follows: section 2 presents the description and modeling of the system under study. In section 3, hybrid system control is presented. Unbalanced load effect on system performance is presented in section 4. To demonstrate the effectiveness of the proposed method, simulation results are presented in section 5. Finally, the paper is concluded in section 6.

2. SYSTEM CONFIGURATION AND MODELING

The purpose of this paper is to use HESS to improve system performance in the presence of the unbalanced load, load changes, and RES power generation changes. As this paper focuses on the overall performances of the HESS, an islanded operated simplified microgrid is taken into consideration. The overall system architecture studied in this paper is shown in Fig.3. The hybrid system in Fig.3 mainly consists of the following elements: a PV power generation system, a battery-SC HESS, DC load and AC load. PV system is considered as main power generator connected to DC bus by a DC-DC boost converter. The maximum power point tracking algorithm is used to control of PV system converter [19]. The Lead-Acid batteries and the SCs are used for hybrid energy storages. The behaviors of the batteries and the SCs are respectively represented by the modified Shepherd curve-fitting model and the Stern model presented in [20]- [21]. In this model, a voltage polarization is added to the battery discharge voltage expression to better representation the effect of the battery state of charge (SOC) on the battery performance. The HESS supports both the steady state as well as transient power changes in generation and loads. The SC supports transient/fluctuating as well as oscillatory power changes and is insufficient to supply/absorb constant power changes (for long time duration) due to its low energy density. While battery support constant power changes due to its high energy density, it may also supply transient power (only under crucial circumstances).

DC load is directly connected to the DC bus. A three-phase inverter is used to connect the AC load to the DC bus. The inverter operates in voltage control mode with fixed frequency obtained from voltage controlled oscillator. Also, traditionally passive filters have been used to remove harmonics from the line current and achieve the desired output AC sinusoidal waveform. The battery and SC units are interfaced with the common DC bus through a bidirectional buck-boost converter. The bidirectional buck-boost converter is capable of operating in buck mode and boost mode. The effective control of the duty cycle of the bidirectional converters assures the rated voltage of the DC bus and the charging and discharging safety of the battery bank and the SC bank. The buck-boost converters topology is shown in Fig. 4 that is composed of a high frequency inductors L_B,L_{sc}, two filtering capacitor $C_{dc}/2$, and four switches S_{11}, S_{12}, S_{13} and S_{14}. The power is transferred from high voltage side to low voltage side (inductor current, $i_L < 0$) when the converter operates in buck mode. Similarly, the power is transferred from low voltage side to high voltage side ($i_L > 0$) when the converter operates in boost mode. The system parameters are presented in Table1.

3. PROPOSED HYBRID SYSTEM CONTROL

The proposed dynamic power management scheme for hybrid system is presented in Fig.5. The power balance in hybrid system is ensured by controlling power at the dc bus. The main purposes of the control strategy are DC bus voltage control as fast as possible under unbalanced load and transient conditions, power sharing between battery and SC to reduce battery current stress as much as possible, faster and better response to transient conditions such as solar radiation changes. By neglecting converter and power line loss; power balance can be expressed as(1).

$$P_L(t) - P_G(t) = P_{bat}(t) + P_{sc}(t) = P_{av}(t) + P_{tran}(t) \quad (1)$$

Where P_G(t) is the power generation of the DGs, P_{bat}(t) is the power flow of the battery, P_L(t) is the power demand of the load, P_{av}(t) is storage average power, P_{tran}(t) is storage transient power, and P_{sc}(t) is the power flow of SC after power conversion by the DC-DC converter. In the outer controller loop, DC bus voltage is compared with the reference voltage and HESS reference currents are generated. To improve performance under unbalanced load changes and transient variations, fuzzy-PI

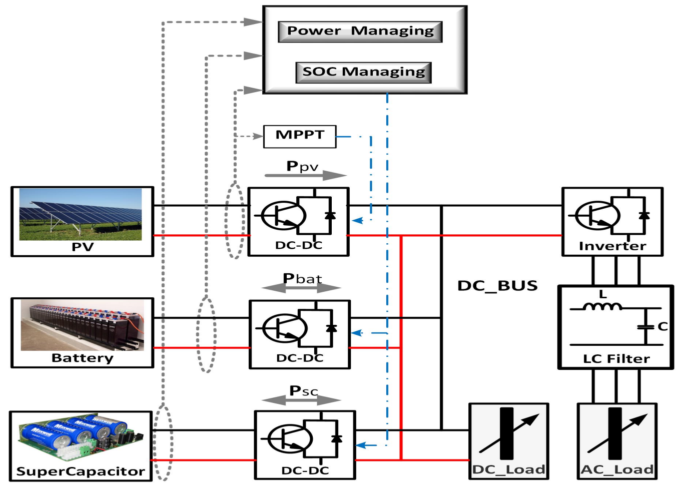

Fig. 3. Hybrid System Under Study.

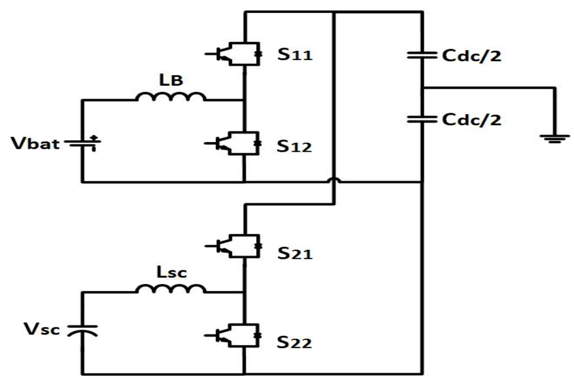

Fig. 4. Bidirectional converter for hybrid energy storage connection and control.

Table 1. System Specification

Parameter	Value	Parameter	Value
V_{dc}	450V	f_{sw}(DC side)	20kHz
$V_{ac}(V_{Line})$	230V	f_{sw}(AC side)	10kHz
V_{bat}	200V	Battery Capacity	100Ah
V_{sc}	200V	SC Capacity	100F
L_{bat}	1mH	Lsc	1mH
PV Nominal power	3kW	C_{dc}	400μF
C_f	50μF	L_f	2mH
AC Line Frequency			50Hz

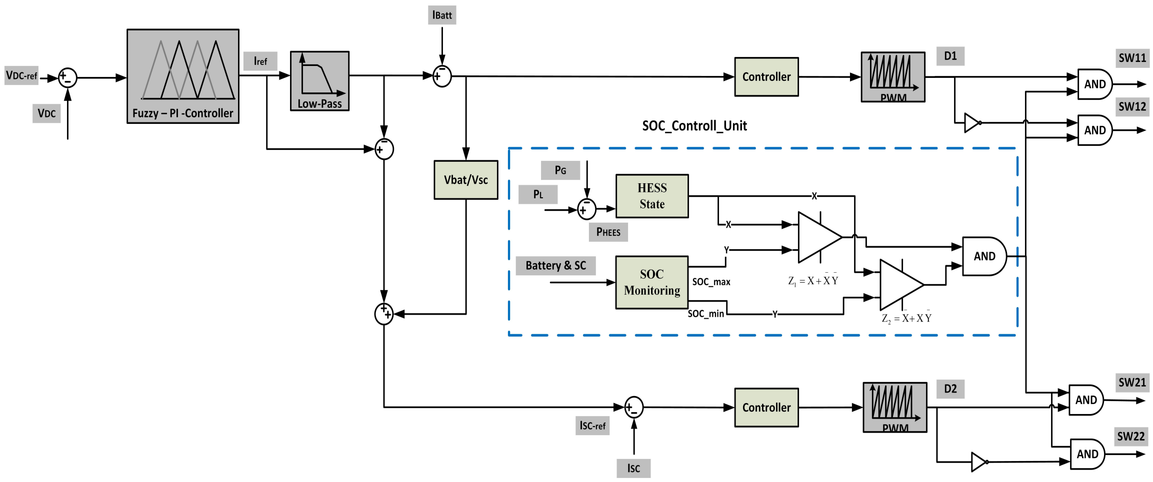

Fig. 5. Hybrid energy storage system control.

controller is used as dc voltage bus controller. HESS reference currents, by using a low pass filter is decomposed into battery and SC reference currents. To reduce battery current stress, battery current error is also added to SC reference current. This control loop causes less stress on the battery. Reference currents of battery and SC are compared with their measured values and by using two PI controller are converted to switching duty ratio (D). Minimum and maximum SOC limitation of HESS are also considered. The HESS state block judges if the HESS should discharge or charge according to the power difference P_{HESS} between the P_L and P_G, with the criterion given as (2).

$$state \begin{cases} 1 \ \ if \ \ P_{HESS} > 0(Discharging) \\ 0 \ \ if \ \ P_{HESS} \leq 0(Charging) \end{cases} \tag{2}$$

The SOC Monitor block monitors the SOC of the Storages by given flag signals $flag_{soc+}$ and $flag_{soc-}$ to indicate whether the SOC has reached the maximum value and minimum value respectively. The values of $flag_{soc+}$ and $flag_{soc-}$ are defined in (3) and(4).

$$flag_{soc+} = \begin{cases} 1 \ \ if \ \ SOC \geq SOC_{\max} \\ 0 \ \ if \ \ SOC < SOC_{\max} \end{cases} \tag{3}$$

and

$$flag_{soc-} = \begin{cases} 1 \ \ if \ \ SOC \leq SOC_{\min} \\ 0 \ \ if \ \ SOC > SOC_{\min} \end{cases} \tag{4}$$

The SOC control system is constructed using logic gates as shown in 5. The block of SOC managing finally is AND with switching pulses. Using this control algorithm, HESS charging and discharging limits are also considered to prevent the destruction of storage devices under deep discharging or overcharging.

A. DC Side Controllers Design

A.1. Battery and SuperCapacitor Controller Design

Fig.6 shows the block diagram of voltage and current controllers. Where (Gc_{bat})is battery current controller transfer function, (G_{bat}) is battery converter transfer function is given as (5), (Gc_{sc}) is SC current controller transfer function, (G_{sc}) is SC converter transfer function, (G_V) is transfer function of inductor current to output voltage, the control transfer function to design the inner current control loop of the battery given as (6).

$$Gc_{bat} = K_P + \frac{K_i}{s} \tag{5}$$

$$G_{bat}(s) = \frac{\hat{i}_b(s)}{\hat{d}(s)} = \frac{(CV_{dc})s + 2(1 - D_{Bat})i_L}{LCs^2 + \frac{L}{R}s + (1 - D_{Bat})^2} \tag{6}$$

where K_p is proportional gain, K_i is integrator gain, C is dc bus capacitor, L is converter inductance, R is load resistance, V_{dc} is dc bus voltage, D_{Bat} is duty ratio, $i_b(s)$ is battery current small perturbations and d(s) is small perturbations in switching duty ratio. SC current loop transfer function is obtained by replacing battery parameters with SC converter parameters in (6). Since the performance of the SC current control loop must be faster than the battery, the SC controller bandwidth will be considered to be 1/6 of switching frequency and the battery bandwidth controller loop considered to be 1/10 of switching frequency. The phase margin of both current controllers is considered to be 60 degrees. The magnitude and phase Bode plot of the open loop transfer function for SC current control loops with and without compensation is shown in Fig.7. Uncompensated and compensated Bode plots for battery control loop are shown in 8. It can be seen that both controllers reduce the resonant peak. Also, it can be seen the phase margin of both controllers is 60 degrees. The table1 parameters are considered for controller design.

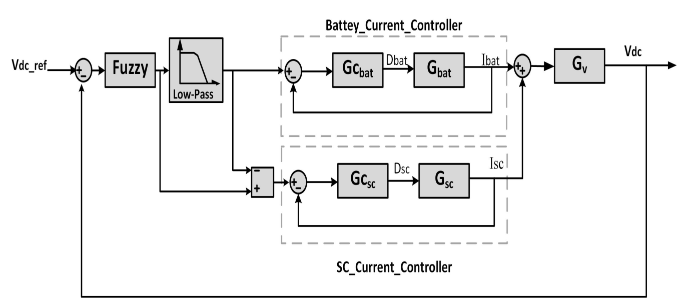

Fig. 6. Control block diagram and transfer functions.

A.2. DC bus Voltage Controller

The DC bus control objective is to regulate the dc bus voltage V_{dc} as accurate and fast as possible under various load variation and unbalanced load conditions. In this study, the fuzzy controller is used in the voltage control loop to compute PI-like actions through fuzzy inference [4]. Fuzzy logic provides a certain level of artificial intelligence to the conventional PI controllers, leading to the effective fuzzy controllers. Fuzzy logic provides fast response times with virtually no overshoot. Loops with noisy process signals have better stability and tighter control when fuzzy logic control is applied [22]. In our approach, the aim is to use a fuzzy controller DC link voltage as fast and accurate as possible in the presence of unbalanced loads and load variations. Therefore, as mentioned above, the main advantages of the fuzzy controller of the PI is better performance in the case of sudden changes and noise signals, so the use of this controller improves the performance of the system. The fuzzy output is used to generate the HESS reference currents. Triangular membership functions are chosen for both of the fuzzy inputs. There are five membership functions for each input, including NB (Negative Big), NS (Negative Small), Z (Zero), PB (Positive Big), and PS (Positive Small). For output, five membership functions, including NB (Negative Big), NS (Negative Small), Z (Zero), PB (Positive Big), and PS (Positive Small) is considered. The fuzzy supervisor rules are obtained from analysing system behavior that is shown in table2.

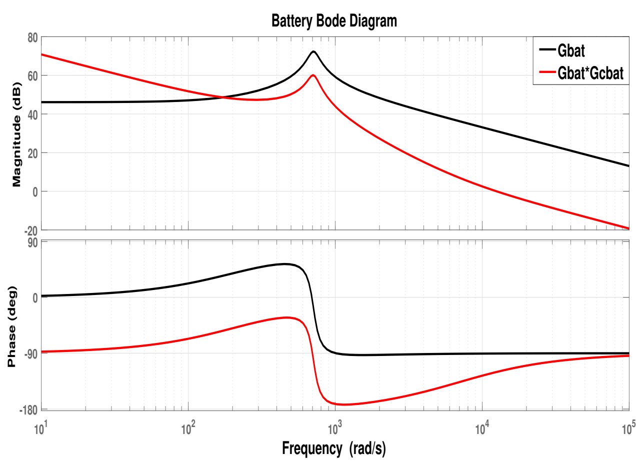

Fig. 7. Battery current controller bode diagram.

Table 2. Fuzzy Controller Rules

	Error					
Delta Error		NB	NS	Z	PS	PB
	NB	NB	NB	NB	Ns	Z
	NS	NB	NB	Z	PS	PB
	Z	NB	NS	Z	PS	PB
	PS	NS	Z	PB	PB	PB
	PB	Z	PS	PB	PB	PB

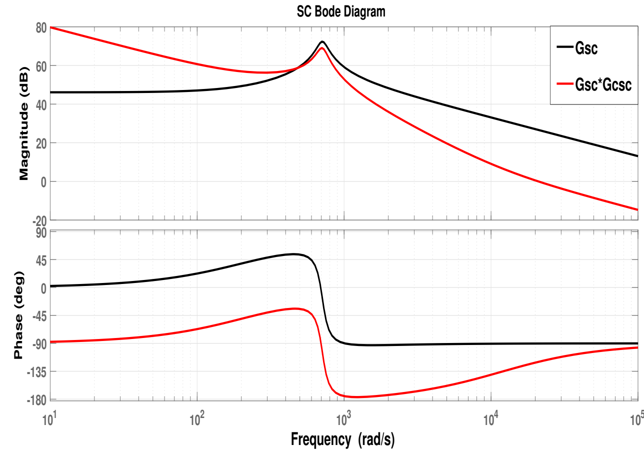

Fig. 8. SC current controller bode diagram.

B. AC Side Controller Design

The proportional-plus-resonant controllers are commonly used, for tracking sinusoidal references as they provide a high gain at the nominal frequency and result in very low steady state error. The transfer function for a PR controller is defined as(7). The Bode plot of the PR controller is presented in Fig.9. It can be seen from Fig.9 that the infinite gain of the ideal transfer function is at the frequency of ω_0, is infinite, and there is no phase shift or gain at other frequencies. PR controller can provide infinite gain at the fundamental frequency which is the reason that PR controller can eliminate steady-state tracking error.

$$G_{PR} = K_{pr} + \frac{2K_r\omega_c s}{s^2 + 2\omega_c s + {\omega_0}^2} \tag{7}$$

where ω_0 denotes the fundamental angular frequency, K_{pr} is the proportional coefficient, K_r is the resonant coefficient, and ω_C is the cut-off frequency. K_{pr} is designed and tuned in the same way of the PI controller, where it aims to achieve the desired phase and gain margins. The PR controller presented in(7) behaves as a high-gain low-pass filter which results in a finite gain and a wider bandwidth. The proposed control block diagram of the AC side controller is shown in Fig.10. The PR controllers are used for the voltage and current control loops and space vector modulation(SVM) switching is used to generate three phase voltage reference.

4. UNBALANCED LOAD EFFECT ON SYSTEM PERFORMANCE

Power electronic converters are used for power conversion. When AC side of an inverter is connected to a nonlinear load, unbalanced load or harmonic load, output power is distorted. This power distortion should be generated by RES and ESS connected to DC bus. Distortion power causes voltage and current deviation in the dc bus. This paper focuses on unbalanced load. For example, the load power of the AC side and the total power drawn from the DC bus for the balanced load and unbalanced load are given in Fig.11. It is clear that the power is distorted when the unbalanced load is added to the system. Regardless of the switching losses, the dc power and ac power are the same. The current and voltage supply by the dc bus is shown in Fig.12. It is clear that dc bus current and voltage have been distorted. SC

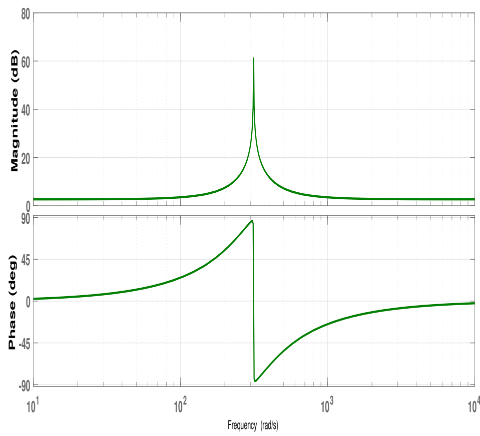

Fig. 9. Inverter current and voltage PR controllers bode diagram.

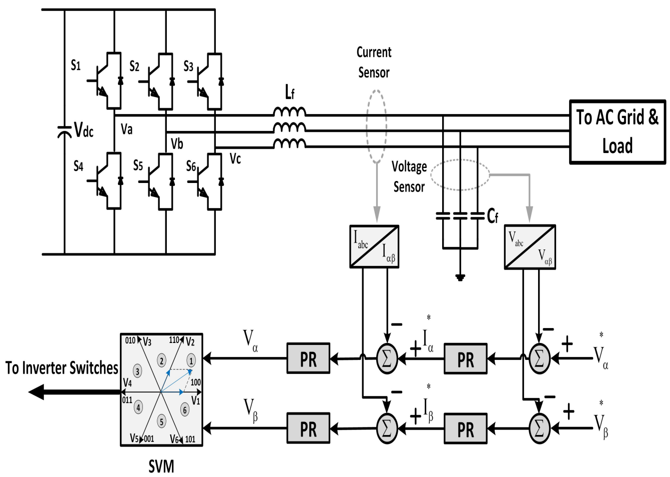

Fig. 10. block diagram of Inverter control.

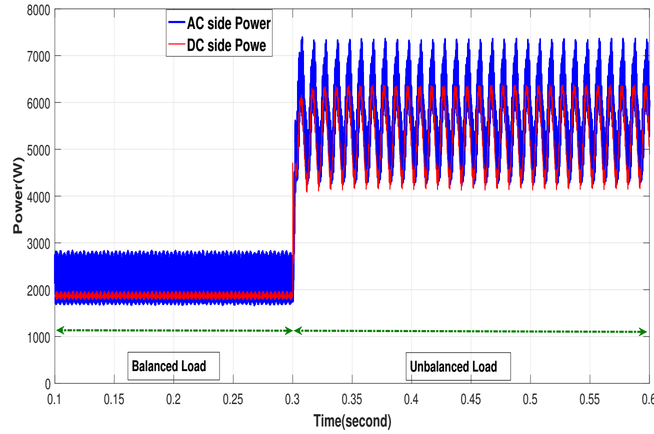

Fig. 11. AC and DC side power under balanced and unbalanced load.

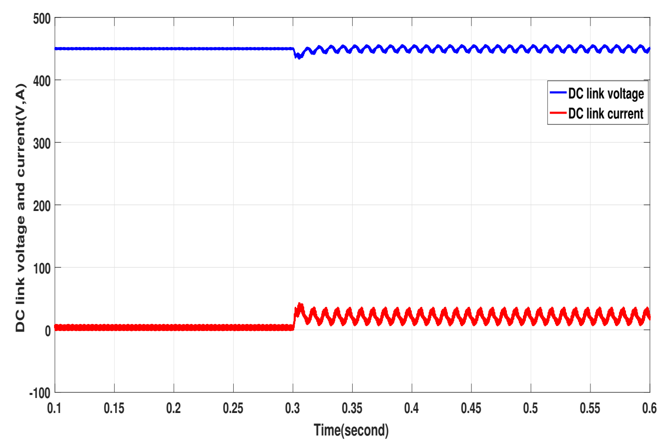

Fig. 12. voltage and current of DC bus.

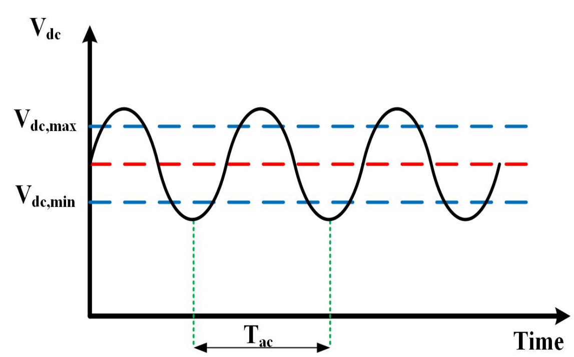

Fig. 13. DC bus voltage with harmonic component [23].

has been used to improve dc bus voltage and current distortion in presence of unbalanced loads and load variations.

The dc bus voltage ripple can be defined as power quality index [23]. Fig.13 shows a DC bus voltage containing a harmonic components with frequency of 1/Tac. If the amplitude of the harmonic content is too large, the ripple of the DC bus can exceed its voltage limits. The DC bus voltage ripple can be defined as(8).

$$\Delta u\% = \frac{V_{dc,\max} - V_{dc,\min}}{V_{dc,\max} + V_{dc,\min}} \quad (8)$$

5. SIMULATION RESULTS

To verify the performance of the proposed control strategy, the system of Fig. 3 has been simulated in MATLAB SIMULINK. To analyze the transient responses of the HESS including the proposed controllers during various load power fluctuation different scenarios are simulated. Parameters used for simulation are presented in Table 1.

A. AC Side Controller

First, PR controllers performance is investigated. To verify the effectiveness of the control method, this method is compared with the conventional classical controller. In this case, the Hybrid system feeds the unbalanced load. The three phase output voltages of inverter are shown in Fig.14 for two control methods.

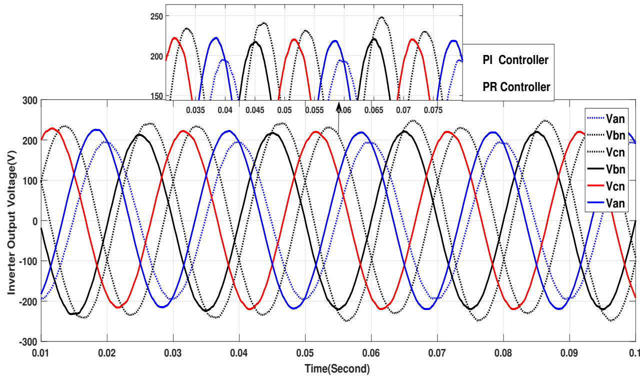

Fig. 14. Inverter output voltages comparison for PR and PI Controller.

It can be seen when the PI controller is used, output voltages are unbalanced but PR controller has better performance under unbalanced load conditions. Using PR controller voltages becomes symmetric but load current remains asymmetric. Unbalanced AC side currents cause disturbances in the currents and voltages of the DC side. Therefore, HESS are used to improve performance.

B. System Performance analysis under unbalanced load conditions

To analyzing proposed system and control algorithm, 3 cases are simulated. In case1 just battery unit is used as storage. In case2 battery and SC are used as storage and PI controllers are selected for dc bus voltage and current control. In this case, DC bus voltage controller is designed such that outer control loop bandwidth is 1/30 of switching frequency and phase margin is 60 degrees. In case3 battery and SC are used as storage and fuzzy-PI controller, described in the previous section, is used as DC bus voltage controller.

In this section, the simulation is done for a step change in DC and AC loads. The hybrid system feeds hybrid DC and AC loads. The initial system load is considered a 2kW AC balanced load. A 2kW DC load is added to the system at t=0.3s. A 1kW single phase load is added to AC side at t=0.5s. By adding the single phase load to the AC side, the load on this side becomes unbalanced. A three phase unbalanced load is added to AC side at t=0.7s. The load power changes are shown in Fig.15. At t=0.5s and t=0.7s the unbalanced load is added to the system. When load is DC or symmetrical AC load, load's power profile is smooth. When unbalanced load is added to the system, power fluctuation is increased. Three phase voltage of AC line is presented in Fig.16. As PR controller is used for inverter control, so three phase voltages remain balanced under unbalanced load conditions. Three phase output currents are shown in Fig.17. From beginning until t=0.5s, loads are balanced, so phase currents are also balanced when, unbalanced load is added to the system, currents become unbalanced. Battery bank currents for three cases are shown in Fig.18. From t=0s to t=0.3s, the load value is smaller than power generated so battery current is negative and the battery bank is charging. As load increases at t=0.3s, t=0.5s and t=0.7s, HESS supply the power difference between generation and load, so it is getting to discharge. It can be seen that battery current with fuzzy controller has variation and more smooth response that increases battery lifetime and qualify system performance. SC currents for two cases are depicted in Fig.19. It can be concluded that control method works well. SC supplies transient and fast variation of requested current. SC current variation for proposed fuzzy method is better than PI method causing fewer battery current stress and better transient response. Fig.20 shows dc bus voltage variation. It can be seen that all controllers have acceptable performance but fuzzy control method has better performance under load variation and transient conditions. The settling time and overshoot, that are very important parameters especially in the hybrid storage system, have been noticeably improved. It is clear that dc bus voltage ripple by using proposed method is about 0.22%, but those are 0.67% and 0.78% in case2 and PI case1 respectively. The results shows the proposed method is very efficient in minimizing the DC bus ripple. Power sharing in the hybrid system for the fuzzy controller is presented in Fig.21. Given the changes in load and the addition of unbalanced loads, it is clear that the proposed control system is well responsive to load variations and the power sharing between the storage devices is well done.

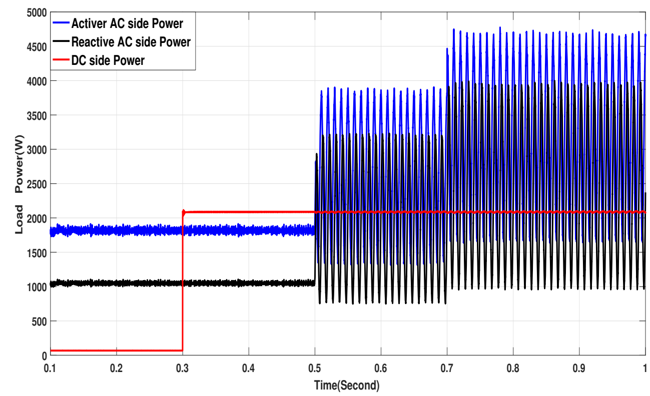

Fig. 15. Load powers for load change.

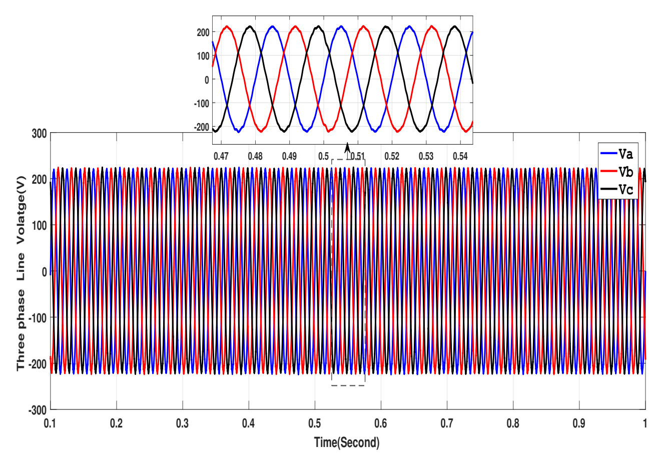

Fig. 16. Inverter output voltage under load changes and unbalanced load conditions.

According to the simulation results, it is clear that when the loads are unbalanced, the distortion current passes through the

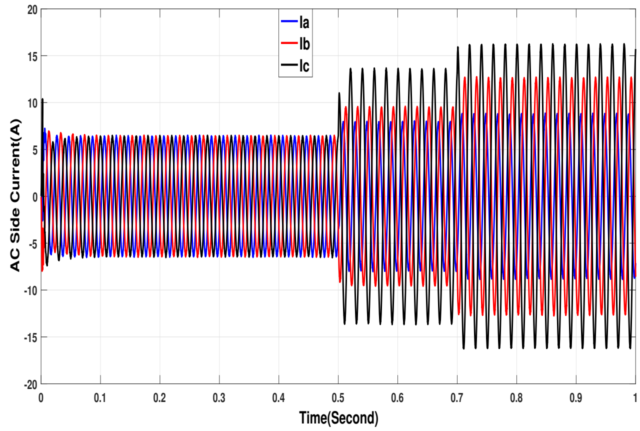

Fig. 17. Inverter output current under load changes and unbalanced load conditions.

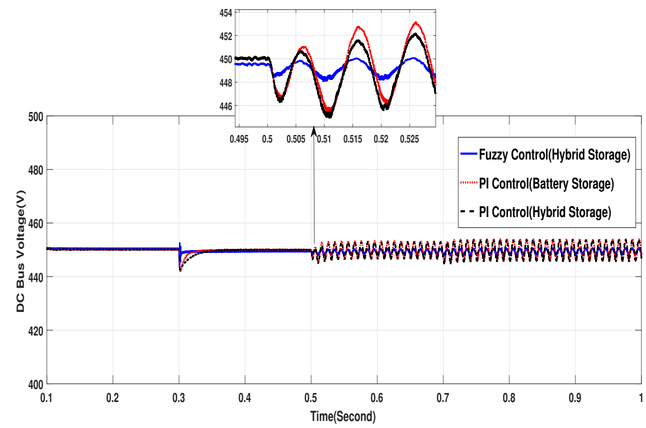

Fig. 20. DC bus voltage under load changes and unbalanced load conditions.

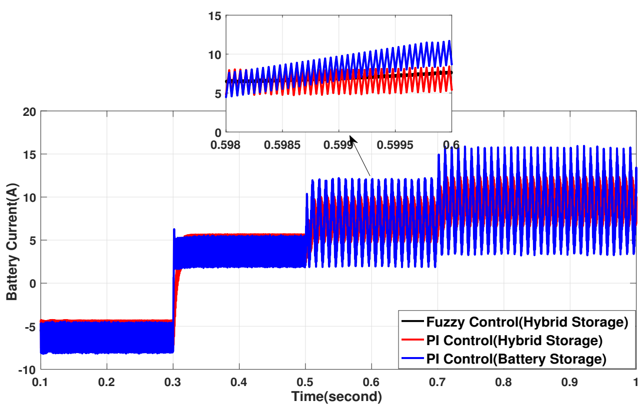

Fig. 18. Battery current under load changes and unbalanced load conditions.

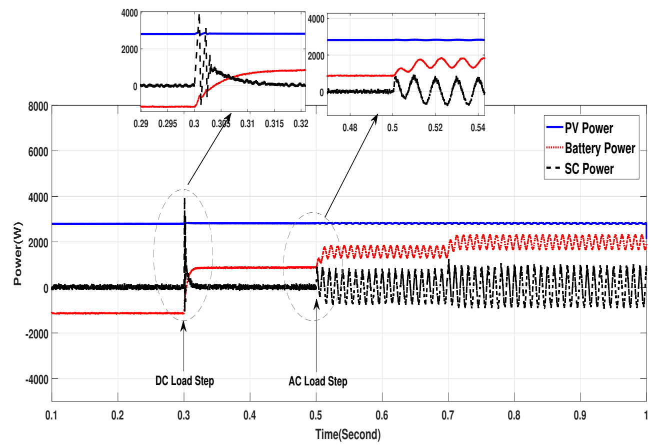

Fig. 21. Power sharing under unbalanced load conditions.

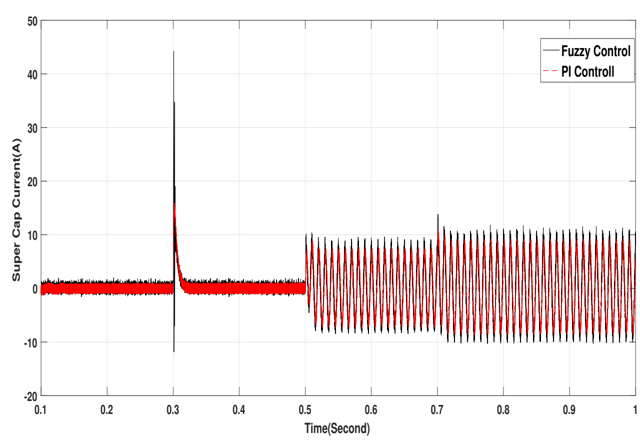

Fig. 19. SC current under load changes and unbalanced load conditions.

DC bus. The control system decomposes this current between storages and PV as follows: SC bank supply the transient current and high-frequency power and battery bank and PV low power frequency, so the power quality of the system improves. Also, according to the results, it is clear that when a sudden change occurs in load under transient condition of the system, a high-density storage device responds well and quickly to these changes, and the performance of the system is improved.

C. Unbalanced load and solar radiation variation

Control system analysis under unbalanced load and solar radiation changes, is presented in this section. At t=0.4s the amount of radiation decreases from 1000(W/m^2) to 700 (W/m^2) and reaches to 900(W/m^2) at the t=0.5s. By solar radiation changing, the amount of power generated by the PV is changed and the control system must do the power sharing correctly. Fig.22 shows the loads power under radiation changes. It is clear that the control system works well and there is no change in the power of the load with solar irradiation changes. Fig.23 shows generation and storage power sharing. By reducing radiation battery and SC must supply power shortage. Battery SOC is shown in Fig.24. Regarding Fig.24 it can be seen when the amount of load is less than the amount of production (P_L<P_G) battery is charging. With load increasing (P_L>P_G), battery is discharged and when PV generation is decreased at t=0.4s SOC slope increase. Given the results of simulations, it can be concluded that the proposed control method works well.

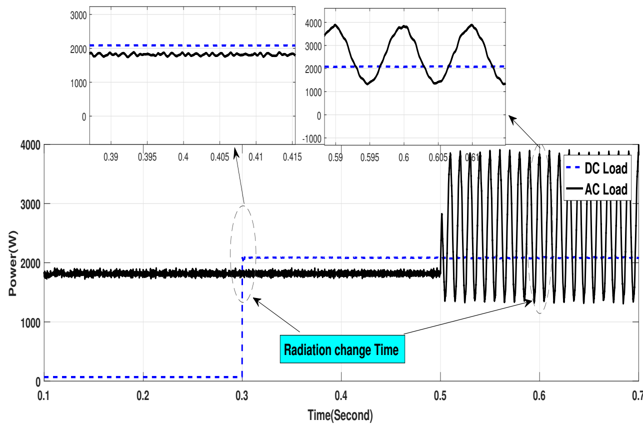

Fig. 22. Load change under radiation changes and unbalanced load conditions.

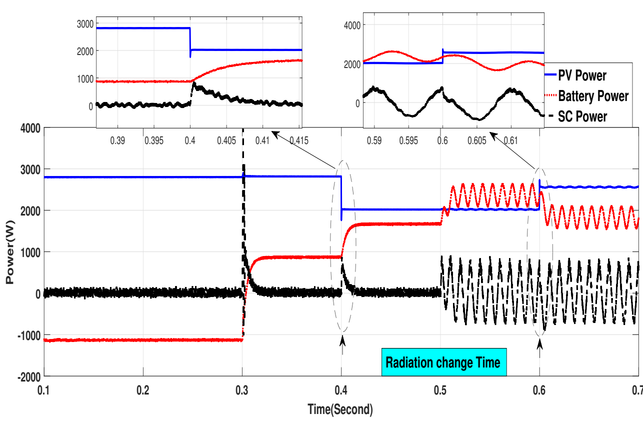

Fig. 23. Power sharing under radiation changes and unbalanced load conditions.

6. CONCLUSION

This paper presents a new approach for power quality improvement by using HESS. The combined utilization of batteries and SCs is the perfect hybridization system of a high energy and high power density. When the loads in microgrid become unbalanced, unbalanced currents causes distortion in the DC bus voltage and current. Using the proposed method and control strategy, the system performance improved and the battery current stress decreased. The main features of the proposed energy management scheme are less stress in the battery system, dynamic power sharing between battery and SC, better DC bus

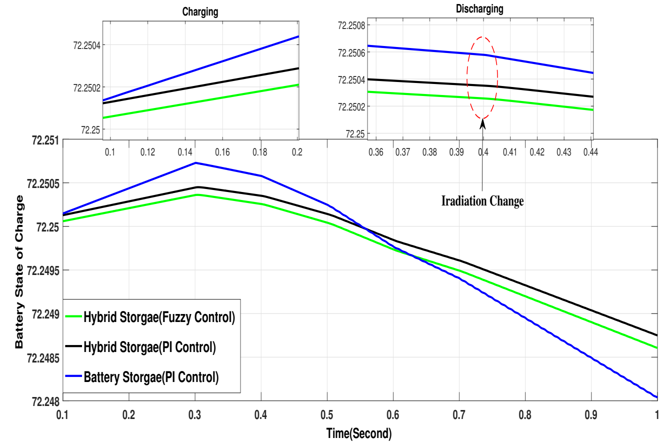

Fig. 24. Battery SOC under radiation changes and unbalanced load conditions.

voltage restoration and to maintain the SOC limits of energy storages within the safe operating region under load change and unbalanced load conditions. The performance of the proposed control approach to reduce the stress in the battery during the normal operation,load change and unbalanced load conditions are also studied. Simulation results in different load conditions prove the effectiveness of the proposed energy management strategy. Moreover, the results verify that the proposed method has good performance under RES generation changes such as solar radiation changing.

REFERENCES

1. H. Bevrani, M. Watanabe, and Y. Mitani, *Microgrid Control: Concepts and Classification*, pp. 288–. Wiley-IEEE Press, 2014.

2. D. W. Gao, "Chapter 3 - interfacing between an {ESS} and a microgrid," in *Energy Storage for Sustainable Microgrid* (D. W. Gao, ed.), pp. 79 – 121, Oxford: Academic Press, 2015.

3. X. Wang, D. Yu, S. L. Blond, Z. Zhao, and P. Wilson, "A novel controller of a battery-supercapacitor hybrid energy storage system for domestic applications," *Energy and Buildings*, vol. 141, no. Supplement C, pp. 167 – 174, 2017.

4. S. Sikkabut, P. Mungporn, C. Ekkaravarodome, N. Bizon, P. Tricoli, B. Nahid-Mobarakeh, S. Pierfederici, B. Davat, and P. Thounthong, "Control of high-energy high-power densities storage devices by li-ion battery and supercapacitor for fuel cell/photovoltaic hybrid power plant for autonomous system applications," *IEEE Transactions on Industry Applications*, vol. 52, pp. 4395–4407, Sept 2016.

5. V. A. Boicea, "Energy storage technologies: The past and the present," *Proceedings of the IEEE*, vol. 102, pp. 1777–1794, Nov 2014.

6. K. Uddin, A. D. Moore, A. Barai, and J. Marco, "The effects of high frequency current ripple on electric vehicle battery performance," *Applied Energy*, vol. 178, pp. 142 – 154, 2016.

7. W. Jing, C. H. Lai, S. H. W. Wong, and M. L. D. Wong, "Battery-supercapacitor hybrid energy storage system in

standalone dc microgrids: areview," *IET Renewable Power Generation*, vol. 11, no. 4, pp. 461–469, 2017.

8. R. A. Dougal, S. Liu, and R. E. White, "Power and life extension of battery-ultracapacitor hybrids," *IEEE Transactions on Components and Packaging Technologies*, vol. 25, pp. 120–131, Mar 2002.

9. J. Cao and A. Emadi, "A new battery/ultracapacitor hybrid energy storage system for electric, hybrid, and plug-in hybrid electric vehicles," *IEEE Transactions on Power Electronics*, vol. 27, pp. 122–132, Jan 2012.

10. Z. Song, H. Hofmann, J. Li, X. Han, X. Zhang, and M. Ouyang, "A comparison study of different semi-active hybrid energy storage system topologies for electric vehicles," *Journal of Power Sources*, vol. 274, no. Supplement C, pp. 400 – 411, 2015.

11. Z. Cabrane, M. Ouassaid, and M. Maaroufi, "Analysis and evaluation of battery-supercapacitor hybrid energy storage system for photovoltaic installation," *International Journal of Hydrogen Energy*, vol. 41, no. 45, pp. 20897 – 20907, 2016.

12. U. Manandhar, N. R. Tummuru, S. Kumar, A. Ukil, G. H. Beng, and K. Chaudhari, "Validation of faster joint control strategy for battery and supercapacitor based energy storage system," *IEEE Transactions on Industrial Electronics*, vol. PP, no. 99, pp. 1–1, 2017.

13. S. K. Kollimalla, M. K. Mishra, and N. L. Narasamma, "Design and analysis of novel control strategy for battery and supercapacitor storage system," *IEEE Transactions on Sustainable Energy*, vol. 5, pp. 1137–1144, Oct 2014.

14. L. W. Chong, Y. W. Wong, R. K. Rajkumar, and D. Isa, "An optimal control strategy for standalone pv system with battery-supercapacitor hybrid energy storage system," *Journal of Power Sources*, vol. 331, no. Supplement C, pp. 553 – 565, 2016.

15. A. Ghazanfari, M. Hamzeh, H. Mokhtari, and H. Karimi, "Active power management of multihybrid fuel cell/supercapacitor power conversion system in a medium voltage microgrid," *IEEE Transactions on Smart Grid*, vol. 3, pp. 1903–1910, Dec 2012.

16. M. Hamzeh, S. Emamian, H. Karimi, and J. Mahseredjian, "Robust control of an islanded microgrid under unbalanced and nonlinear load conditions," *IEEE Journal of Emerging and Selected Topics in Power Electronics*, vol. 4, pp. 512–520, June 2016.

17. Y. Zhu, F. Zhuo, and F. Wang, "Coordination control of lithium battery-supercapacitor hybrid energy storage system in a microgrid under unbalanced load condition," in *2014 16th European Conference on Power Electronics and Applications*, pp. 1–10, Aug 2014.

18. Q. Tabart, I. Vechiu, A. Etxeberria, and S. Bacha, "Hybrid energy storage system microgrids integration for power quality improvement using four-leg three-level npc inverter and second-order sliding mode control," *IEEE Transactions on Industrial Electronics*, vol. 65, pp. 424–435, Jan 2018.

19. M. Rakhshan, N. Vafamand, M. H. Khooban, and F. blaabjerg, "Maximum power point tracking control of photovoltaic systems: A polynomial fuzzy model-based approach," *IEEE Journal of Emerging and Selected Topics in Power Electronics*, vol. PP, no. 99, pp. 1–1, 2017.

20. Q. Li, H. Yang, Y. Han, M. Li, and W. Chen, "A state machine strategy based on droop control for an energy management system of pemfc-battery-supercapacitor hybrid tramway," *International Journal of Hydrogen Energy*, vol. 41, no. 36, pp. 16148 – 16159, 2016. Special Issue: 16th China Hydrogen Energy Conference (CHEC 2015), November 2015, Zhenjiang City, Jiangsu Province, China.

21. O. Tremblay and L.-A. Dessaint, "Experimental validation of a battery dynamic model for ev applications," *World Electric Vehicle Journal*, vol. 3, no. 1, pp. 1–10, 2009.

22. A. I. Al-Odienat and A. A. Al-Lawama, "The Advantages of PID Fuzzy Controllers Over The Conventional Types," *American Journal of Applied Sciences*, vol. 5, pp. 653–658, jun 2008.

23. K. T. Mok, M. H. Wang, S. C. Tan, and S. Y. R. Hui, "Dc electric springs x2014;a technology for stabilizing dc power distribution systems," *IEEE Transactions on Power Electronics*, vol. 32, pp. 1088–1105, Feb 2017.